Perpendicular Magnetic Anisotropy in Fe–N Thin Films: Threshold Field for Irreversible Magnetic Stripe Domain Rotation

Louis Charles Garnier, Mahmoud Eddrieff, Samuele Fin, D. Bisero, Franck Fortuna, Victor H. Etgens, Massimiliano Marangolo

SPIN
Vol. 6, No. 4 (2016) 1640014 (8 pages)

DOI: 10.1142/S2010324716400142

World Scientific
www.worldscientific.com

Perpendicular Magnetic Anisotropy in Fe–N Thin Films: Threshold Field for Irreversible Magnetic Stripe Domain Rotation

L.-C. Garnier[*,†,††], M. Eddrief[*], S. Fin[‡], D. Bisero[‡,§], F. Fortuna[¶,‖], V. H. Etgens[*,†,**] and M. Marangolo[*]

[*]*Sorbonne Universités*
UPMC Université Paris 06, CNRS
Institut des NanoSciences de Paris
4 Place Jussieu, F-75005 Paris, France

[†]*Université Versailles St-Quentin, LISV*
Bâtiment Boucher, Pôle Scientifique et Technologique de Vélizy
10-12 Avenue de l'Europe, F-78140 Vélizy, France

[‡]*Dipartimento di Fisica e Scienze della Terra*
Università degli Studi di Ferrara
Via Saragat 1, I-44122 Ferrara, Italy

[§]*CNISM, Unità di Ferrara*
I-44122 Ferrara, Italy

[¶]*Univ Paris-Sud, CSNSM, UMR 8609*
Bâtiments 104 et 108, F-91405 Orsay, France

[‖]*CNRS, IN2P3*
F-91405 Orsay, France

[**]*Institut VEDECOM*
77 rue des Chantiers, F-78000 Versailles, France
[††]*louis-charles.garnier@insp.upmc.fr*

Received 21 November 2016
Accepted 23 January 2017
Published 22 February 2017

The magnetic properties of an iron nitride thin film obtained by ion implantation have been investigated. N_2^+ ions were implanted in a pristine iron layer epitaxially grown on ZnSe/GaAs (001). X-ray diffraction measurements revealed the formation of body-centered tetragonal N-martensite whose c-axis is perpendicular to the thin film plane and c-parameter is close to that of α'-Fe_8N. Magnetic measurements disclosed a weak perpendicular magnetic anisotropy (PMA) whose energy density K_{PMA} was assessed to about $10^5\,J/m^3$. A sharp decline of the in-plane magnetocrystalline anisotropy (MCA) was also observed, in comparison with the body-centered cubic iron. The origin of the PMA is attributed to the MCA of N-martensite and/or stress-induced anisotropy. As a result of the PMA, weak magnetic stripe domains with a period of about 130 nm aligned along the last saturating magnetic field direction were observed at remanence by magnetic

force microscopy. The application of an increasing in-plane magnetic field transverse to the stripes H_{trans} highlighted a threshold value ($\mu_0 H_{\text{trans}} \approx 0.1\,\text{T}$) above which these magnetic domains irreversibly rotated. Interestingly, below this threshold, the stripes do not rotate, leading to a zero remanent magnetization along the direction of the applied field. The interest of this system for magnetization dynamics is discussed.

Keywords: Magnetic thin films; perpendicular magnetic anisotropy; weak magnetic stripe domains; iron nitrides; nitrogen-martensite; ion implantation.

1. Introduction

Among ferromagnetic iron nitrides, metastable N-martensite forms interstitial compounds with a body-centered tetragonal (bct) structure and can accommodate a nitrogen concentration of up to ≈ 13 at.%.[1] In principle, this tetragonal distortion of the body-centered cubic (bcc) α-Fe lattice leads to a large magnetocrystalline anisotropy MCA due to the reduced crystal symmetry. It was shown that thin films constituted of N-martensite with (001) texture, made by ion implantation,[2] sputtering[3,4] or molecular beam epitaxy (MBE),[5] exhibit a perpendicular magnetic anisotropy (PMA). This effect becomes strong when the nitrogen concentration is close to that of α'-Fe_8N and increases with N site ordering associated to the presence of the chemically ordered α''-$Fe_{16}N_2$.[3,5] It is worth noting that α''-$Fe_{16}N_2$ has been studied for decades owing to its possible, but controversial giant saturation magnetization[6] and large MCA.[5] Such magnetic properties could make it a promising candidate for next generation rare-earth-free magnets.[7] However, it was also reported that lattice expansion of N-martensite leads to a large increase of the average magnetic moment per iron atom without requiring any additional ordering of the nitrogen atoms.[4] In this paper, we report on the modifications of the crystalline structure and magnetic properties induced by nitrogen implantation in an iron thin film. We highlight the presence of weak magnetic stripe domains due to the appearance of PMA in a layer with N-martensite. We also show that those stripes can be easily rotated by applying a magnetic field above a threshold value. Concerning spin dynamics, PMA materials have been studied for applications in the field of spintronics.[8,9] N-martensite have notably attracted attention as potential ferromagnetic electrodes for future spintronic devices.[3] Besides, it is interesting to note that weak magnetic stripe domains can play an important role in magnonics. Indeed, peculiar resonance modes can be easily excited by a judicious application of an external varying magnetic field as pointed out by Ebels *et al.*[10] Very rich dynamic susceptibility spectra characterized by surface modes and strongly confined volume modes have been observed and calculated in systems very similar to ours.[11,12] This work will pave the way for extensive studies on magnetization (and spin) dynamics in N-martensite thin films for spintronic and magnonic applications.

2. Material and Methods

The iron thin film used as ion implantation target with a thickness of 78 nm was deposited by MBE on a ZnSe-buffered GaAs(001) substrate. The presence of the ZnSe buffer layer prevents chemical reactions between iron and the semiconductor substrate.[13,14] The main in-plane crystallographic directions attested by reflection high-energy electron diffraction measurements are α-Fe [110] // ZnSe [110] // GaAs [110] and α-Fe [100] // ZnSe [100] // GaAs [100]. Then, the film was protected against oxidization by an 8-nm-thick gold capping layer. Ion implantation was performed at room temperature with nitrogen molecular ions N_2^+ accelerated to 40 keV with a fluence of 5.3×10^{16} ions/cm^2. The ion current density was kept below 5.5 μA/cm^2 and the target was not cooled during the implantation. The ion beam was perpendicular to the sample surface and the channeling effect in the iron film was not taken into account due to the gold capping layer. The depth profile of nitrogen in the sample implanted was simulated using the transport of ions in matter (TRIM) simulation program.[15] The ion energy was determined so that nitrogen was implanted throughout the thickness of the iron thin film. The indicated fluence value is that of the sample with the strongest PMA which has been made. Measurements of X-ray diffraction (XRD)

patterns of the as-grown and as-implanted samples were carried out using monochromatized Cu Kα radiation in a high-resolution SmartLab diffractometer. The magnetization curves were measured at room temperature by a vibrating sample magnetometer (VSM) after a careful calibration of the instrument. The saturation magnetization was determined with an experimental error due to the volume measurement of the samples. The thicknesses of the unimplanted and implanted iron layers were investigated by X-ray reflectometry (XRR). The magnetic domain structure was explored by magnetic force microscopy (MFM).[16,17]

3. Results and Discussion

3.1. *Structural investigations*

Figure 1 shows XRD patterns in the out-of-plane direction of as-grown and as-implanted samples. For the unimplanted sample, the α-Fe (002) line reveals the strong [001] preferred orientation of the epitaxial iron thin film perpendicular to the film plane. After nitrogen implantation, an asymmetric peak with a shoulder at higher angles discloses the iron nitride formation. This peak was assigned as the α'–Fe–N (002) reflection based on the currently available knowledge of iron nitrides crystallographic structures and the results of in-plane XRD measurements (discussed later in this section). Here, the designation α'–Fe–N refers to N-martensite with a ratio of nitrogen to iron atoms of less than 1/8. The basic structure of N-martensite was described as a bcc

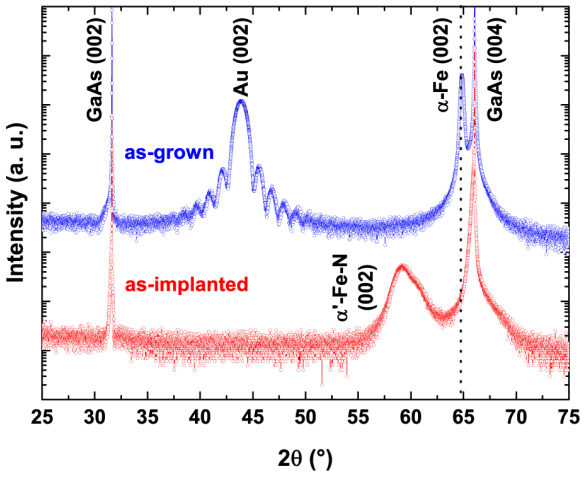

Fig. 1. XRD patterns of an as-grown sample and an as-implanted sample.

iron lattice elongated along the c-axis with nitrogen atoms at the octahedral interstices.[1] Besides, it was shown that the unit cell parameter along the c-axis becomes larger when the nitrogen concentration increases.[1] The position of the peak's maximum intensity of α'–Fe–N (002) is found at $2\theta = 59.27°$, it can be inferred a c lattice constant of 3.12 Å, following the Bragg's law. Based on the literature, the distortion and the nitrogen concentration of the nitride formed are slightly lower than those of bct α'-Fe_8N whose (002) planes' scattering angle is $2\theta = 58.66°$.[1] The α'–Fe–N (002) peak width reflects the low crystalline quality of the nitrogen implantation induced compound. Besides, the nitrogen concentration is not uniformly distributed throughout the iron layer thickness according to the profile simulated using TRIM.[15] The observed shoulder is believed to result from the formation of a minority α'–Fe–N with less nitrogen. The α-Fe (002) line disappearance is due to a decrease in iron accompanied with nitride formation. No diffraction lines of α'–Fe–N other than those from the c planes were observed. Hence, the N-martensite c-axis is oriented along the perpendicular to the film plane [001] direction. Ion implantation induced a sputtering effect and resulted in a surface recession of the protecting gold layer. The fact that the Au (002) line is not observable after implantation means most of the gold protection layer was sputtered. However, no diffraction lines of iron oxides were observed. Moreover, ion implantation in a multilayer can lead to interface mixing. The strength of this effect has been assessed considering the recoil atom distributions from a second TRIM simulation.[15] Nitrogen in a gold-capped iron thin film under our experimental conditions leads to a mixing area of about 2 nm on each side of the interface between the gold and iron layers. In the case that solid solutions of gold and iron were formed, their influence would be negligible due to their low proportions.

Additional XRD measurements were performed along the in-plane directions [100] and [110] of the GaAs(001) substrate for the pristine and implanted thin films. For the as-grown sample, the (200) and (220) diffraction peaks of α-Fe insure the epitaxy of the iron layer. For the as-implanted sample, peaks assigned as α'–Fe–N (200) and (220) have been found at the same diffraction angles as the α-Fe (200) and (220) lines considering the error bar (not reported here). The formed iron nitride has in-plane lattice parameters close to those of α-Fe and

maintains the in-plane crystallographic orientations of the iron layer.

Nitrogen ion implantation in the iron thin film has resulted in the formation of [001] oriented bct N-martensite with the same in-plane lattice parameters as α-Fe (considering the experimental error bar) and an out-of-plane lattice parameter close to the c-lattice constant of α'-Fe_8N. This selective formation by nitrogen implantation in epitaxial iron thin film of N-martensite with their c-axis oriented perpendicularly to the film has already been noted and discussed by Nakajima *et al.*[2]

3.2. *Magnetic measurements*

Figure 2 compares the magnetization curves taken along in-plane crystallographic directions [100], [110] and out-of-plane crystallographic direction [001], for the nitrogen-implanted iron thin film and the as-grown iron thin film in the inset. Before nitrogen implantation, the expected behavior of an iron thin film is observed. The hardest axis is along the out-of-plane direction [001] because of the thin film shape anisotropy. The easiest axis is along the in-plane direction [100] due to the bcc iron MCA. After nitrogen implantation, the out-of-plane direction is still the hardest axis, but the in-plane magnetic behavior becomes isotropic. In addition, the in-plane magnetic loops show a qualitative difference in shape with respect to the unimplanted sample ones. The coercivity H_c and the saturation field H_s increase ($\mu_0 H_c = 2.5 \times 10^{-2}$ T; $\mu_0 H_s = 3.5 \times 10^{-1}$ T), the ratio of the remanence and saturation magnetization M_r/M_s decreases ($M_r/M_s = 0.39$) and the saturation magnetization M_s remains constant within the error bar ($M_s = 1.7 \pm 0.2$ MA/m). They also display a region where the magnetization changes linearly with the applied magnetic field. As we will see below, this behavior is a fingerprint of stripe-like domain patterns in thin films.[18] It is well known that iron nitride formation and ion implantation lattice damages can cause strong magnetic changes. However, it should be noted that the in-plane magnetic loops are very similar to those shown by Ji *et al.* and Dirba *et al.* for N-martensite thin films made by sputtering.[3,4] They especially reported a correlation between the saturation magnetic field and the average c lattice constant determined by XRD and our values are consistent with the observed trend despite the fact that we used a different method of sample preparation. Nevertheless, we did not observe the increase of the saturation magnetization induced by the lattice expansion reported by Dirba *et al.*[4] Notwithstanding that we also carefully determined the thin films thickness by XRR (low film roughness for the implanted sample), we consider our larger experimental error bar to be more realistic.

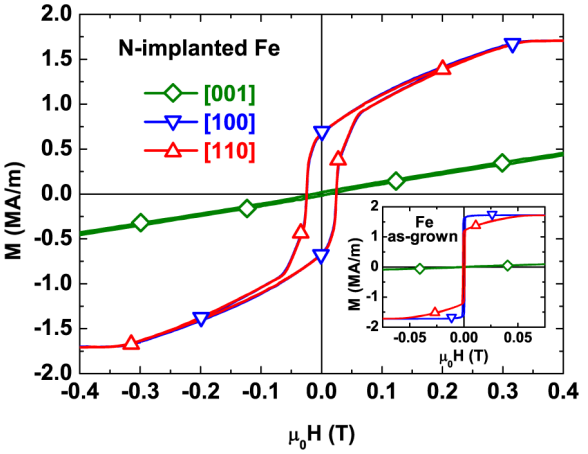

Fig. 2. Magnetization curves for a nitrogen-implanted iron thin film and an as-grown iron thin film in the inset, measured by VSM. The field was applied along the out-of-plane [001] direction and the in-plane [100] and [110] directions.

In Fig. 3, we compare the magnetization curves taken along the out-of-plane direction [001] before and after nitrogen implantation. In this configuration, H_s corresponds to the effective anisotropy field H_A, for all the anisotropies perpendicular to the film plane whatever their origin, and is dependent on M_s. For the as-grown iron thin film, the shape anisotropy is only taken into account. In the case of the nitrogen-implanted iron thin film, there is a decrease of H_A without change of M_s which indicates that PMA is induced by nitrogen implantation. This PMA may originate from the MCA of α'-Fe-N with their longer axis perpendicular to the thin film and from stress-induced anisotropy due to ion implantation.[2] In the first approximation, adding a uniaxial anisotropy term in the expression of the thin film magnetic energy, the perpendicular energy density K_{PMA} can be estimated from M_s and H_A values. K_{PMA} is found to be of about 10^5 J/m^3 and is of the same order of magnitude as those reported for the MCA constant of α'-Fe_8N made by sputtering[3] and MBE.[5] This K_{PMA} value has been confirmed by ferromagnetic resonance (FMR) measurements, the results of which are the subject of a separate study.

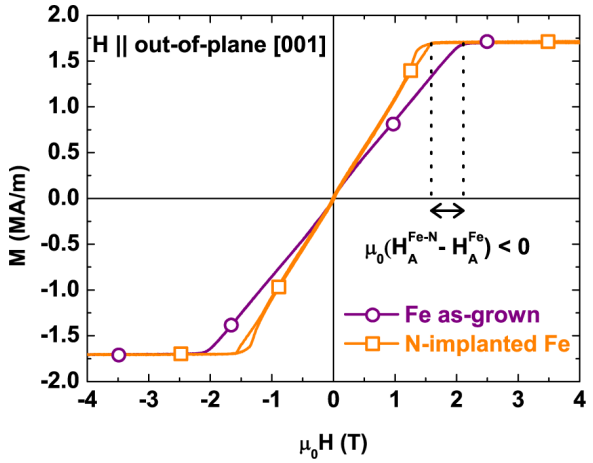

Fig. 3. Magnetization curves for the iron and nitrogen-implanted iron thin films, measured by VSM. The field was applied along the out-of-plane [001] direction.

Determining the ratio between the PMA constant K_{PMA} and the demagnetizing energy $1/2\mu_0 M_s^2$ for the thin film, we obtained a quality parameter $Q = K_{\mathrm{PMA}}/1/2\mu_0 M_s^2 < 1$ indicating that the PMA is weak. In this case, the weak magnetic stripe domain structure is favored, provided that the film thickness is larger than a critical value as shown in Fe–Ga[19,20] and FePt[21] thin films. Parallel stripe magnetic domains are continuous micromagnetic structures and appear at remanence with a perpendicular magnetization component having a periodic modulation alternately upwards and downwards.[22] The stripes were found in Fe/Fe–N multilayers,[23] Fe–N single layers[24] and were expected by Takahashi *et al.* in α''-$Fe_{16}N_2$ thin film grown by MBE, but were not observed for technical reasons.[25] In order to explore this particular effect in a thin film with N-martensite, we performed MFM measurements using the phase-detection mode.[26]

Magnetic stripe domains at remanence and aligned along the direction of the last saturating field are shown in Fig. 4(a). From the fast Fourier transform of the image [Fig. 4(b)], we found that the period of the pattern is about 130 nm. When we applied a saturating magnetic field in other directions, we observed that the whole stripe pattern rotates parallel to the last saturating field direction. This reorientation is irreversible since, when the magnetic field is removed, the stripe structure is preserved. This behavior is observed in systems with rotatable anisotropy,[21] and was reported in permalloy[27] and Fe–N thin films.[24]

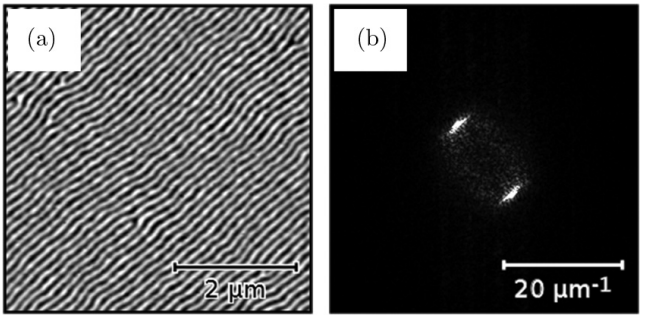

Fig. 4. (a) MFM image of the as-implanted sample taken at remanence, after saturation along the [100] direction. (b) 2D Fast Fourier Transform of the MFM image.

We also carried out MFM measurements at remanence after applying an increasing field H_{trans} in plane along the direction perpendicular to the stripes in order to observe the different steps of their reorientation. Firstly, after aligning the stripes along [110] with a saturating field, we observed that the orientation of the domain structure is preserved for $\mu_0 \mathrm{H}_{\mathrm{trans}} < 0.08\,\mathrm{T}$. Secondly, after aligning the stripes along [100] with a saturating field [Fig. 5(a)], these magnetic domains rotate coherently abruptly through an angle of about 60° for $\mu_0 H_{\mathrm{trans}} = 0.1\,\mathrm{T}$ [Fig. 5(b)]. For higher fields, the angle of rotation

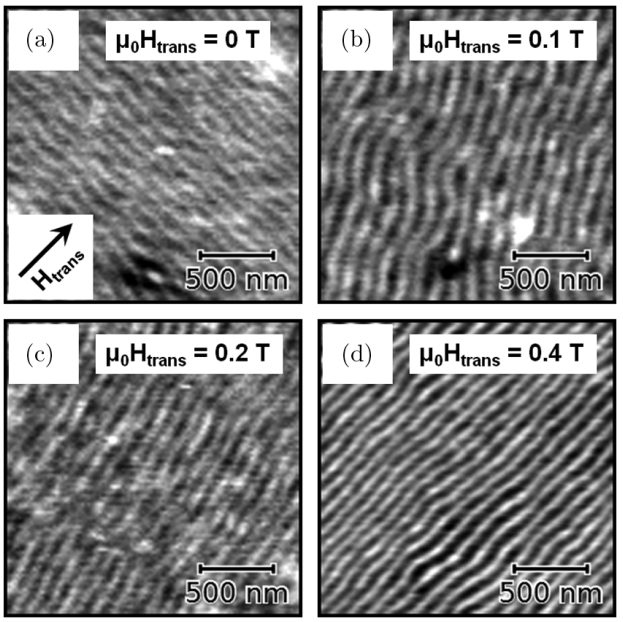

Fig. 5. MFM images taken at remanence with the stripes (a) aligned along the [100] direction by a saturating magnetic field, and after applying an in-plane transversal magnetic field $\mathrm{H}_{\mathrm{trans}}$ with (b) $\mu_0 H_{\mathrm{trans}} = 0.1\,\mathrm{T}$, (c) $\mu_0 H_{\mathrm{trans}} = 0.2\,\mathrm{T}$, (d) $\mu_0 H_{\mathrm{trans}} = 0.4\,\mathrm{T}$.

increases gradually [Figs. 5(c) and 5(d)], and a complete reorientation is attained for $\mu_0 H_{\text{trans}} = 0.4\,\text{T}$ [Fig. 5(d)]. These MFM measurements show a threshold to rotate the stripes for $\mu_0 \text{H}_{\text{trans}}$ between 0.08 T and 0.1 T.

In order to have additional details on the rotation threshold of the magnetic stripe domains, specific VSM measurements were performed on the nitrogen-implanted sample. A saturating field was first applied in plane to align the stripes along the [110] direction and was removed. Then, a magnetic field H_{trans} transverse to the stripes direction was applied and reduced to zero while the component of the magnetization along the direction of H_{trans} was recorded. As shown in Fig. 6(a), this two-step measurement was repeated many times, each time increasing the maximum value of H_{trans}, up to the saturation field. Finally, a complete hysteresis loop was measured. As shown in Fig. 6(b), the evolution of the in-field magnetization M_{on} and the remanent magnetization M_{off}, as a function of the maximum H_{trans} value, are different. However, for each curve, two trends are distinguished for H_{trans} lower and higher than a threshold value ($\mu_0 H_{\text{trans}} \approx 0.1\,\text{T}$) which is consistent with the rotation threshold of the magnetic stripe domains. For $\mu_0 H_{\text{trans}} < 0.1\,\text{T}$, M_{on} goes up whereas M_{off} stays close to zero. The magnetization orientation in the sample is reversible and the stripes are still perpendicular to the measurement direction at remanence. For $\mu_0 H_{\text{trans}} \approx 0.1\,\text{T}$, M_{on} and M_{off} rise sharply. However, this disruption is more important for M_{off} which reaches about 76% of its value after applying a saturating field. The magnetization of the sample becomes irreversible and the stripes rotate through a large angle. For $\mu_0 H_{\text{trans}} > 0.1\,\text{T}$, M_{on} increases at a lower rate, and M_{off} grows up very slightly in general. The stripes rotate until they are aligned along the applied field direction. A similar behavior was observed in $\text{Fe}_{1-x}\text{Ga}_x$ thin films grown on ZnSe/GaAs(001).[20] It was suggested that the reversible behavior originates from the expanding and shrinking abilities of partial-flux-closure cap domains parallel to the external field. In our case, a varying nitrogen concentration depth profile in the thin film may lead to the low dispersion of measured out-of-plane lattice constant values of α'-Fe–N (cf. Sec. 3.1). Hence, a variation of PMA as a function of the thin film depth may exist. This PMA depth profile may contribute to the magnetic stripe domain rotation experimentally observed.

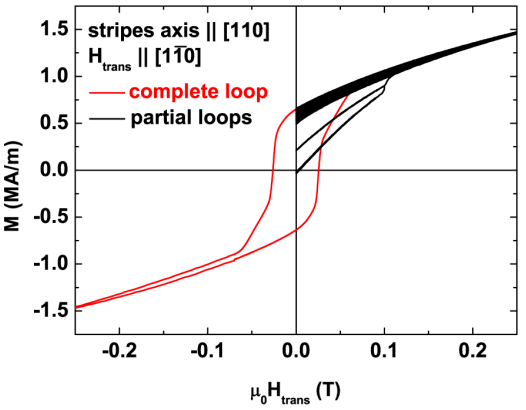

(a)

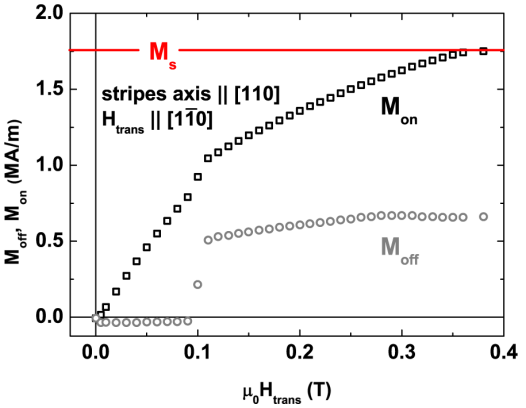

(b)

Fig. 6. VSM measurements of the component of the magnetization along the in-plane magnetic field applied perpendicularly to the stripes. The stripes were aligned along the [110] direction by a saturating magnetic field beforehand. (a) The different partial loops refer to different values of the maximum intensity of the applied field. A complete loop was subsequently recorded. (b) Evolution of the magnetization under field (M_{on}) and at remanence (M_{off}) as a function of $\mu_0 H_{\text{trans}}$.

3.3. *Perspectives concerning magnetization dynamics*

Fe–N thin films with PMA are of great interest concerning magnetization dynamics. Weak magnetic stripe domain structures present a wealth of interesting resonance modes, unlike strong magnetic stripe domain structures where alternately upwards and downwards uniformly (or almost uniformly) magnetized domains are separated by thin Bloch-type walls. Indeed, in addition to the expected acoustic and optic domain resonances, domain walls and flux-closure caps give rise to new specific modes.[10] Besides, multiple resonances associated with surface and volume modes of stripe domains

can be observed, when the magnetization is unsaturated, by broad band FMR experiments and reproduced by micromagnetic simulations.[11,12] Another approach to the study of weak magnetic stripe domains is about local dynamics of topological defects which is promising for technological applications and contributes to the exploration of the nanoscale physics of topological spin states. Future spintronics devices may use mobile particle-like magnetic entities as functional objects such as skyrmions.[28] In addition, Dussaux *et al.* recently shown in FeGe that the depinning and subsequent motion of magnetic edge dislocations are involved in the collective movements of the helical spin texture that propagates over mesoscopic length scales.[29]

4. Conclusions

In conclusion, we have carried out a magnetic study of a nitrogen-implanted iron thin film epitaxially grown on ZnSe/GaAs(001). We have shown that nitrogen implantation causes selective formation of bct N-martensite whose c-axis is oriented perpendicularly to the thin film plane and c-parameter is close to that of α'-Fe_8N. Strong changes are observed in the magnetic properties of the thin film. In-plane magnetic measurements have shown an increase of the coercivity and of the saturation field, a decrease of the remanent magnetization and a loss of the in-plane magnetic anisotropy. A PMA appeared and was found to be of about $10^5\,\mathrm{J/m^3}$. The causes for this PMA may be the magnetic anisotropy of the bct nitride and stress-induced anisotropy. We highlight that this weak PMA favors a magnetic stripe domain structure. Besides, we performed a study of the rotation of the stripes by applying a transverse magnetic field H_{trans} and we measured a rotation threshold for $\mu_0 H_{\mathrm{trans}} \approx 0.1\,\mathrm{T}$ by both MFM and VSM. Our research on stripe domains has led to ongoing studies on magnetic anisotropies, magnetization dynamics and the field-dependent behavior of topological defects in nitrogen-martensite thin films.

Acknowledgment

We would like to express our appreciation to Paola Atkinson for preparing the GaAs substrate by MBE, Dominique Ledu for doing the implantation, Sarah Hidki for carrying out XRD investigations, Jean-Marc Dubus for his cooperation and Laura Thevenard for a careful reading of the manuscript. This work is funded by the MATINNOV industrial chair (ANR-12-CHIN-0004) of the French National Research Agency (ANR), resulting from the collaboration between the University of Versailles Saint-Quentin-en-Yvelines and VALEO. Support from the PICS-2013 SWIM joint research program between CNR (Italy) and CNRS (France), the SPINSAW project (ANR-13-JS04-0001-01), the PRIN2010 (2010ECA8P3) and FIRB2010 (RBFR10E61T) projects of the Italian Ministry of Education, Universities and Research (MIUR) are gratefully acknowledged.

References

1. K. H. Jack, *Proc. R. Soc. Lond. A* **208**, 200 (1951).
2. K. Nakajima and S. Okamoto, *Appl. Phys. Lett.* **56**, 92 (1990).
3. N. Ji, M. S. Osofsky, V. Lauter, L. F. Allard, X. Li, K. L. Jensen, H. Ambaye, E. Lara-Curzio and J.-P. Wang, *Phys. Rev. B* **84**, 245310 (2011).
4. I. Dirba, P. Komissinskyi, O. Gutfleisch and L. Alff, *J. Appl. Phys.* **117**, 173911 (2015).
5. H. Takahashi, M. Igarashi, A. Kaneko, H. Miyajima and Y. Sugita, *IEEE Trans. Mag.* **35**, 2982 (1999).
6. M. Takahashi and H. Shoji, *J. Magn. Magn. Mater.* **208**, 145 (2000).
7. J.-P. Wang, S. He and Y. Jiang, Iron nitride permanent magnet and technique for forming iron nitride permanent magnet U. S. patent application 14/238,835 (2014).
8. S. Mangin, D. Ravelosona, J. A. Katine, M. J. Carey, B. D. Terris and E. E. Fullerton, *Nat. Mater.* **5**, 210 (2006).
9. H. Meng and J. P. Wang, *Appl. Phys. Lett.* **88**, 172506 (2006).
10. U. Ebels, L. D. Buda, K. Ounadjela and P. E. Wigen, Small Amplitude Dynamics of Nonhomogeneous Magnetization Distributions: The Excitation Spectrum of Stripe Domains. in *Spin Dynamics in Confined Magnetic Structures I*, eds. B. Hillebrands and K. Ounadjela (Springer-Verlag, Berlin, 2002), pp. 167–217.
11. N. Vukadinovic, O. Vacus, M. Labrune, O. Archer and D. Pain, *Phys. Rev. Lett.* **85**, 2817 (2000).
12. N. Vukadinovic, M. Labrune, J. Ben Youssef, A. Marty, J. C. Toussaint and H. Le Gall, *Phys. Rev. B* **65**, 054403 (2001).

13. M. Marangolo, F. Gustavsson, M. Eddrief, Ph. Sainctavit, V. H. Etgens, V. Cros, F. Petroff, J. M. George, P. Bencok and N. B. Brookes, *Phys. Rev. Lett.* **88**, 217202 (2002).
14. M. Eddrief, M. Marangolo, S. Corlevi, G.-M. Guichar, V. H. Etgens, R. Mattana, D. H. Mosca and F. Sirotti, *Appl. Phys. Lett.* **81**, 4553 (2002).
15. J. F. Ziegler, J. P. Biersac and U. Littmark, *The Stopping and Range of Ions in Solids* (Pergamon, New York, 1985).
16. D. Bisero, P. Cremon, M. Madami, M. Sepioni, S. Tacchi, G. Gubbiotti, G. Carlotti, A. O. Adeyeye, N. Singh and S. Goolaup, *J. Nanopart. Res.* **13**, 5691 (2011).
17. M. Sepioni, M. Madami, S. Tacchi, G. Gubbiotti, G. Carlotti, D. Bisero, A. O. Adeyeye, N. Singh and S. Goolaup, *J. Phys.: Conf. Ser.* **200**, 072089 (2010).
18. N. Saito, H. Fujiwara and Y. Sugita, *J. Phys. Soc. Jpn.* **19**, 1116 (1964).
19. M. Barturen, B. Rache Salles, P. Schio, J. Milano, A. Butera, S. Bustingorry, C. Ramos, A. J. A. de Oliveira, M. Eddrief, E. Lacaze, F. Gendron, V. H. Etgens and M. Marangolo, *Appl. Phys. Lett.* **101**, 092404 (2012).
20. S. Fin, R. Tomasello, D. Bisero, M. Marangolo, M. Sacchi, H. Popescu, M. Eddrief, C. Hepburn, G. Finocchio, M. Carpentieri, A. Rettori, M. G. Pini and S. Tacchi, *Phys. Rev. B* **92**, 224411 (2015).
21. E. Sallica Leva, R. C. Valente, F. Martinez Tabares, M. Vasquez Mansilla, S. Roshdestwensky and A. Butera, *Phys. Rev. B* **82**, 144410 (2010).
22. A. Hubert and R. Schäfer, *Magnetic Domains: The Analysis of Magnetic Microstructures* (Springer, Berlin, 1998).
23. W. Szuszkiewicz, K. Franc, B. Hennion, F. Ott and M. Aleszkiewicz, *J. Alloys Compd.* **423**, 172 (2006).
24. K. Sin and S. X. Wang, *IEEE Trans. Mag.* **33**, 2833 (1997).
25. H. Takahashi, K. Mitsuoka, M. Komuro and Y. Sugita, *J. Appl. Phys.* **73**, 6060 (1993).
26. G. Gubbiotti, P. Malagò, S. Fin, S. Tacchi, L. Giovannini, D. Bisero, M. Madami, G. Carlotti, J. Ding, A. O. Adeyeye and R. Zivieri, *Phys. Rev. B* **90**, 024419 (2014).
27. J. Wei, Z. Zhu, H. Feng, J. Du, Q. Liu and J. Wang, *J. Phys. D: Appl. Phys.* **48**, 465001 (2015).
28. R. Tomasello, E. Martinez, R. Zivieri, L. Torres, M. Carpentieri and G. Finocchio, *Sci. Rep.* **4**, 6784 (2014).
29. A. Dussaux, P. Schoenherr, K. Koumpouras, J. Chico, K. Chang, L. Lorenzelli, N. Kanazawa, Y. Tokura, M. Garst, A. Bergman, C. L. Degen and D. Meier, *Nat. Commun.* **7**, 12430 (2016).